WCCM V
Fifth World Congress on
Computational Mechanics
July 7-12, 2002, Vienna, Austria
Eds.: H.A. Mang, F.G. Rammerstorfer,
J. Eberhardsteiner

Parallel Implementation and Development of a Probabilistic Model for 3D Discrete Concrete Cracking

C. N. M. Paz, L. F. Martha

Department of Civil Engineering
Pontifical Catholic University of Rio de Janeiro (PUC-Rio) - Brazil
e-mail: {mena,lfm}@tecgraf.puc-rio.br

E. M. R. Fairbairn, J. L. D. Alves*, N. F. F. Ebecken and A. L. G. A. Coutinho

COPPE/UFRJ - Program of Civil Engineering
C.P. 68506, 21945-970
Federal University of Rio de Janeiro – Brazil
e-mail:eduardo@labest.coc.ufrj.br, jalves@lamce.ufrj.br , nelson@ntt.ufrj.br , alvaro@nacad.ufrj.br

Key words: Concrete cracking, probabilistic crack approach, heterogeneity, parallel computing

Abstract

This work presents a probabilistic crack approach (Rossi *et al* [1]), based on the Monte Carlo method, that was recently implemented in a 3D fully parallelized finite element code (Paz, [2]). The cracking scheme used is the discrete crack approach introduced by 3D interface elements. In this approach the heterogeneity of the material is taken into account by considering the properties to vary spatially following a normal distribution determined by the mean the standard deviation of the considered material properties. *N* samples of a vector of these properties are generated and the corresponding solutions are computed by the FE code. Hence, the average response of the *N* samples corresponding to a Monte Carlo simulation is a function of the mean value and of the standard deviation that define the Gauss density function. If the heterogeneous characteristics of the material are well established and quantified by the statistical moments it is possible that the model displays the size effects related to the material heterogeneity.

Fracturing is modeled by 3D interface elements generated in a previously defined region within the mesh. The interface elements are triangular base prisms connecting adjacent faces of neighboring tetrahedra. These elements simulate crack opening through relative displacements between the triangular faces (Paz [2]).

1. Introduction: Probabilistic Model

Among several other relevant factors, such as water/cement ratio of the paste, casting and curing conditions, loading conditions, etc. concrete cracking depends on the random distribution of constituents and initial defects. The heterogeneity governs the overall cracking behavior and related size effects on concrete fracture. The probabilistic crack approach, based on the direct Monte Carlo method, developed by Rossi and co-workers [1] takes this stochastic process into account by assigning in finite element analysis, randomly distributed material properties (tensile strength, Young's modulus) to both the solid elements and the contact elements. The stochastic process is introduced at the local scale of the material, by considering that cracks are created within the concrete with different energy dissipation depending on the spatial distribution of constituents and initial defects. The local material behavior in concrete is assumed to obey a perfect elastic brittle behavior, so that the random distribution of local cracking energies can be replaced by a random distribution of local strengths. Therefore, solid elements are elastic, while interface elements are considered elastic-brittle.

The present probabilistic model involves a number of mechanic properties of the material to be determined, which constitutes the modeling data. From a large number of direct tensile tests it was found that a normal law describes rather well the experimental distribution (Rossi *et al.* [1]). These characteristics are: $f_{ct,m}$ and E_m, the means of the tensile strength and of the Young's modulus respectively; $f_{ct,s}$ and E_s, the standard deviations of the tensile strength and of the Young's modulus respectively. The following analytical expressions were proposed:

$$f_{ct,m} = 6.5\,(V_t / V_g)^{-a}; \qquad f_{ct,s} / f_{ct,am} = 0.35\,(V_t / V_g)^{-b} \tag{1}$$

$$E_m = E \qquad E_s / E = 0.15\,(V_t / V_g)^{-c} \tag{2}$$

where V_t is the volume of the two finite elements contiguous to an individual contact element of the mesh; V_g is the volume of the coarsest aggregate; E is the average Young's modulus that does not exhibit significant volume effects. For cylinder specimens, whose dimensions are 160 mm in diameter and 320 mm high *a*, *b* and *c* are constants related to it's compressive strength f_c given by:

$$\begin{aligned} a &= 0.25 - 3{,}6\times10^{-3}(f_c) + 1.3\times10^{-5}(f_c)^2 \\ b &= 4.5\times10^{-2} + 4.5\times10^{-3}(f_c) - 1.8\times10^{-5}(f_c)^2 \\ c &= 0.116 + 2.7\times10^{-3}(f_c) - 3.4\times10^{-6}(f_c)^2 \end{aligned} \tag{3}$$

In these expressions, the compressive strength f_c represents the quality of the concrete matrix, while the volume of the coarsest aggregate V_g, refers to the elementary material heterogeneity.

Equations (1) to (3) show that the smaller the scale of observation, the larger the fluctuation of the local mechanical properties, and thus the (modeled) heterogeneity of the matter. In other words, the finer the mesh, the greater the modeled heterogeneity in terms of Young's modulus and tensile strength.

The mesh has m_v tetrahedra elements and m_i interface elements. The individual Young's modulus of the tetrahedra elements is referenced by $\mathbf{E}_{iv}$ and the elastic-brittle constitutive law of the interface elements is characterized by an individual tensile strength $\mathbf{f}_{ct,ii}$.

Following Rossi *et al*. [1] findings these individual local tensile strengths and Young's modulus are represented by normal distributions having the densities:

$$g_f(f_{ct}) = \frac{1}{f_{ct,s}\sqrt{2p}} \exp\left[-\frac{1}{2}\left(\frac{f_{ct,m}}{f_{ct,s}}\right)^2\right] \tag{4}$$

$$g_E(E) = \frac{1}{E_s\sqrt{2p}} \exp\left[-\frac{1}{2}\left(\frac{E - E_m}{E_s}\right)^2\right] \tag{5}$$

where $g_f(f_{ct})$ and $g_E(E)$ are density functions for the tensile strength f_{ct} and the Young's modulus E, respectively, and x_m and x_s denote the mean and standard derivation of the distribution of quantity x. For the problem at hand, it is possible to find a sample of m_i values $\mathbf{f}_{ct,ii}$, each value corresponding to an interface element, and m_v values $\mathbf{E}_{iv}$, each value corresponding to a volume element, by using a standard routine for generation of random numbers for a given normal distribution (Press *et al.*, [3]).

The problem with this approach is that these statistical moments are not known, a priori, for the characteristic volume of the finite elements used in analysis. However, some methods have been proposed to determine these parameters by means of inverse analysis using neural networks [2], [4], [5]and [6].

The solution for this probabilistic approach is obtained by means of a Monte Carlo simulation (depicted in fig 1). A number of n samples are generated (for a given normal distribution) and some characteristic responses of the structure (for example, stress crack-width $s - w$ curve, or load displacement $P - d$ curve, or load crack mouth opening displacement $P - CMOD$ curve) are computed.

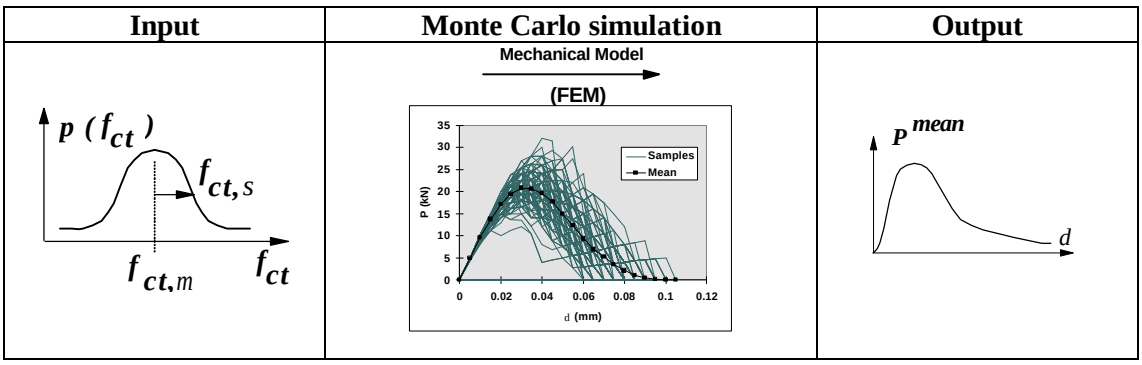

Figure1: Monte Carlo simulation

2. Discrete cracking: 3D Interface elements

The finite element cracking model is a discrete model for which volume elements are always elastic and cracking occurs in elastic-brittle (almost rigid brittle) contact elements placed between two volume elements. The 3D interface elements (Paz [2]) depicted in Fig. 2 (a) can be thought as triangular base prisms connecting adjacent faces of neighboring tetrahedra.

These elements are formulated to represent relative displacements between the triangular faces to simulate crack opening.

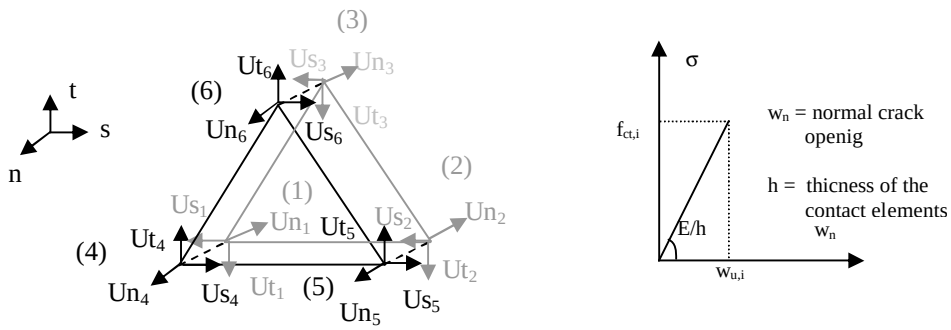

(a) (b)

Figure 2: (a) An Interface Element and its degrees of freedom in a local system, (b) Elastic-Brittle Contact law

The constituve law of the 3D interface element is defined by equation (6) for non cracked elastic state, characterized by $s_n < f_{ct,i}$. When the tensile strength is exeeded, the elements reach a cracked stage and module E_c and G_c are set to zero (fig. 2 (b)).

$$? \mathbf{s} = \mathbf{D}_{cr}\ \Delta \mathbf{w} = \begin{Bmatrix} \Delta s_n \\ \Delta s_s \\ \Delta s_t \end{Bmatrix} = \begin{bmatrix} E_{c/h} & 0 & 0 \\ 0 & G_c/h & 0 \\ 0 & 0 & G_c/h \end{bmatrix} \begin{Bmatrix} \Delta w_n \\ \Delta w_s \\ \Delta w_t \end{Bmatrix} \tag{6}$$

In equation (6) the subscripts *n*, *s* and *t* indicate the directions normal and transversal to the crack plane respectively, *w* are the relative displacements between the two faces of the interface element, *h* is the width of interface element, E_c and G_c are the longitudinal (Young's) and the transversal modulus respectively.

Equation (6) and fig. 2(b) define the elasto-brittle constituve behavior. However, it can be considered rigid-fragile, since thickness *h* of the interface element is considered very small (less than a value $h_{\lim}$) of such form that the solution of the problem does not get excited if *h* diminishes, $h < h_{\lim}$. In this way the modulus E_c and G_c in equation (6) does not have a physical meaning and the terms E_c/h and G_c/h tend to infinity.

The kinematic relation for the interface element is given by:

$$\Delta \mathbf{w} = \mathbf{B}\, \Delta \mathbf{a}_l^e \tag{7}$$

The stiffness matrix for the interface element is by:

$$\mathbf{K}_{\mathrm{Intf}}^{\mathrm{e}} = \int_{\Omega} \mathbf{B}^T\ \mathbf{D}_{cr} \mathbf{B}\, \mathrm{d}\Omega \tag{8}$$

The interface elements are automatically generated (Paz [2]) contiguous to the faces of selected tetrahedra. This selection is performed by the user defining a 3D box inside the mesh that contains the target elements.

3. Implementation code strategies, parallel vector processor (PVP)

3.1. Solution of equilibrium equations and the inexact Newton Method

In this paper we employ an Inexact Newton method (Kelley, [7]), to solve large-scale three dimensional incremental elastic-brittle problems. In the Inexact Newton Method, at each nonlinear iteration, a linear system of finite element equations is approximately solved by the preconditioned conjugate gradient method (PCG).
In the finite element method, the implementation of global matrix-vector products are easily parallelized in different computer architectures, performing element level products followed by global assembly. This type of implementation is often referred to element-by-element (EBE) scheme. Matrix-vector products computed by EBE (Hughes [8]) schemes are memory intensive, requiring more operations than the product with the assembled matrix, because element matrices have many overlapping non-zero entries.
When solving iteratively the finite element system of linear equations, it is straightforward to employ inexact versions of the standard Newton-like methods (Kelley, [7], Papadrakakis, [9]). In this case, tolerances for the inner iterative driver may be adaptively selected to minimize computational effort towards the solution, giving rise to the following algorithm:

Given u_{tol}, r_{tol}, h_i relative and residual tolerance.

Compute stiffness tetrahedra matrix $\mathbf{K}_{Tetra}$

do k=1,2….., number of load increments do

Compute external forces vector

$$\mathbf{F}_{ext}^{k} = \mathbf{F}_{nodal}^{K} + \mathbf{F}_{volume} + \mathbf{F}_{\bar{s}} - \left(\mathbf{K}_{tetra}\, \bar{\mathbf{U}}_k + \mathbf{K}_{Intef}\, \bar{\mathbf{U}}_k \right)$$

do i=1,2 ..., while convergence

Compute internal forces vector,

$$\mathbf{F}_{\text{int}}^{i} = \left(\mathbf{F}_{\text{int}}^{i} \right)_{Tetra} + \left(\mathbf{F}_{\text{int}}^{i} \right)_{Intf}$$

Compute residual vector,

$$\mathbf{?}^{\,i} = \mathbf{F}_{\text{int}}^{i} - \mathbf{F}_{ext}^{i}$$

Update stiffness interface matrix $\mathbf{K}_{\text{Intf}}^{\text{i}}$

$$\mathbf{A}^{i} = \mathbf{K}_{Tetra} + \mathbf{K}_{Intf}^{i}$$

Compute tolerance for iterative driver, h_i

Solver: $\mathbf{A}^{i}\ \Delta\mathbf{u} = \mathbf{?}^{\,i}$ for tolerance h_i

Update solution,

$$\mathbf{U} = \mathbf{U} + \Delta\mathbf{u}$$

if $\dfrac{\| \Delta\mathbf{u} \|}{\| \mathbf{U} \|} \le utol$ and $\dfrac{\| \Delta\mathbf{?}^{\,i} \|}{\| \mathbf{F}_{ext}^{k} \|} \le rtol$ then convergence

end while i.

end do k.

Note that in $\mathbf{F}_{ext}^{k}$ we account for nodal forces, body forces and prescribed displacements and stresses $\bar{\mathbf{u}}, \bar{\mathbf{s}}$. The total internal forces vector $\mathbf{F}_{\text{int}}^{i}$ is the sum of the tetrahedra element vector internal forces $\left(\mathbf{F}_{\text{int}}^{i}\right)_{Tetra}$ plus the interface element internal forces vector $\left(\mathbf{F}_{\text{int}}^{i}\right)_{Intf}$. The total stiffness matrix is the sum of the continuum matrix $\mathbf{K}_{Tetra}$ plus the inteface matrix $\mathbf{K}_{Intf}^{i}$ update at each nonlinear iteration.
We adopted a simple nodal block-diagonal preconditioner. Therefore, the most expensive computational kernel in the linear solver is the matrix-vector product.
According to the above algorithm, an approximate solution is obtained when the Inexact Newton termination criterion is satisfied, that is, when,

$$\left\| \mathbf{A}^{i}\ \Delta\mathbf{u} - \Psi^{i} \right\| \leq h_{i} \left\| \Psi^{i} \right\| \tag{9}$$

The tolerance h_i may be selected using Papadrakakis, [9] or Kelley [7].

3.2 Matrix-vector products element-by-element, EBE

In the element-by-element EBE matrix-vector product, the matrix $\mathbf{A}$ it is never formed. Rather, the product is computed as:

$$\mathbf{A}\,\mathbf{p} = \sum_{e=1}^{Nel} \mathbf{A}_e\mathbf{p} = \sum_{i=1}^{N_{tetra}} \left(\mathbf{K}_{Tetra}\ \ \mathbf{p}_i\right) + \sum_{i=1}^{N_{Intf}} \left(\mathbf{K}_{Intf}\ \ \mathbf{p}_i\right) \tag{10}$$

where *Nel* is the number of elements in the mesh, N_{tetra} is the number of tetrahedra, N_{intf} is the number of interface elements, $\mathbf{A}_e$ are the element matrices for the tetrahedra and interface; $\mathbf{p}_e$ the components of $\mathbf{p}$ restricted to the degrees of freedom of the element. The arrays of the element stiffness matrices are stored taking into account their symmetry; in the case of the element tetrahedra 78 coefficients are stored and for the interface element only 18 coefficients are stored, exploring the particular structure of the discrete gradient operator (matrix **B**).
Note that, during the nonlinear iterations, only the interface elements stiffness matrices should be updated.
The mesh coloring algorithm Hughes [8] was extended in order to block both solid and interface into disjoint groups this enabling full vectorization and parallelism of the operations involved in equation (10).

4. Numerical simulation and comparison with experimental data

A notched, plain concrete three-point bending beam test carried out at Amparano *et al* [10]. The geometrical details of the test are shown in fig. 3 and fig. 4 with the mesh of tetraedra of 3D interface element. The thickness of beam is 63.5 mm, which was determined by considering the maximum aggregate, size 19 mm. To examine the effect of maximum aggregate content, a volume fraction of 55% of aggregate to total concrete volume was considered. Tests on specimens made whit this concrete indicated the following average characteristics at the age (28 days) the model were tested; $f_{ct} = 3{,}45\,MPa$ and $E_c = 10500\,MPa$. This model was created by MG modeler [11] using J-mesh algorithm [12]. Interface elements were later included in the model using the algorithm developed in (Paz [2]).

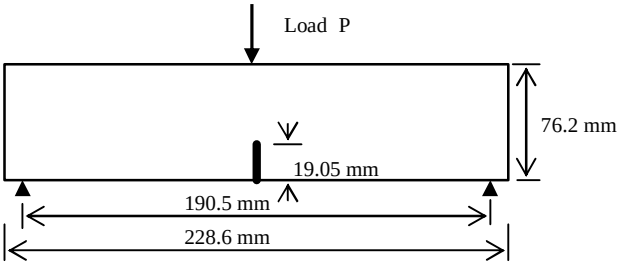

Figure 3: Specimen geometry for the three-point bend beam

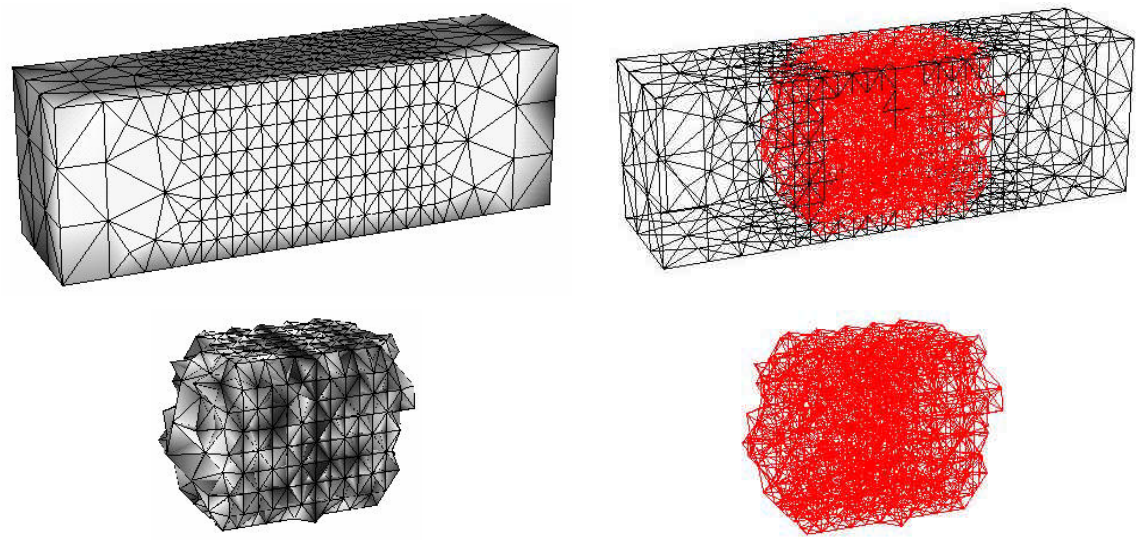

Figure 4: Mesh of tetraedra with interface elements and detail for the mesh of interface elements

Tipical Load-CMOD (crack mouth opening displacement) curves, obtained from numerical simulation, and comparison of experimental and numerical results are shown in fig. 5.

Fig. 6 presents the crack configurations for given sample at a stage corresponding to de softening branch of the Load-CMOD curve.

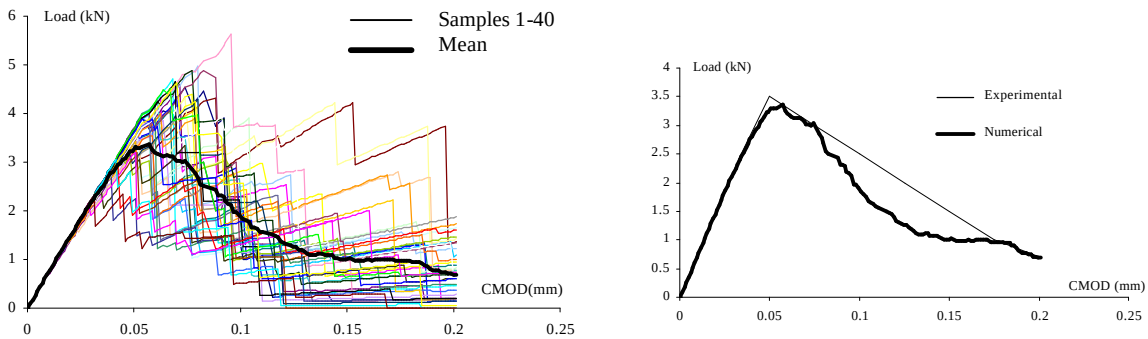

(a) (b)

Figure 5: (a) Monte Carlo simulation
(b) Comparison of experimental and numerical results

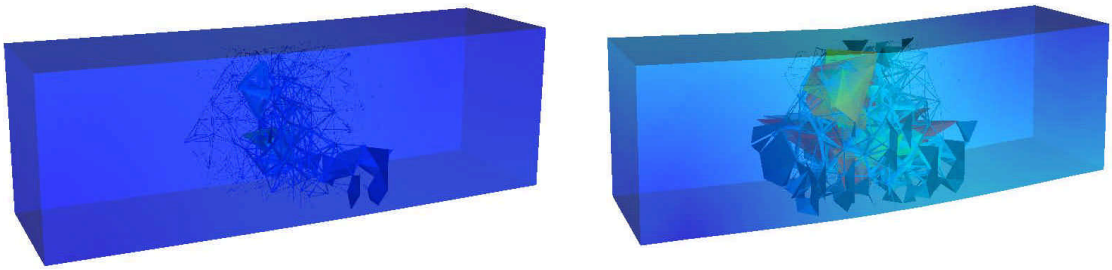

Figure 6: Crack evolution for numerical simulation.

5 Computational Performance

Vector performance analysis was obtained using the program summary provided by PERFVIEW's Report as shown showed in tab. 1. The CPU time of the vectorized single processor run for CRAY T90 is 33.99 hours. This table relates the single CPU utilization to the Mflop/s rates for the three top routines. The routines **Smatv-fint** and **Smatv-tetra** are responsible respectively for the matrix-vector operations on the interface elements and tetrahedra element, these multiplications are needed in the routine **PCG-block,** the iterative driver to the implementing the nodal block diagonal preconditioned Conjugate Gradient Method (PCG).

Table 1: Performance Analysis -The top 3 subroutines

Routines	Single CPU (%)	Performance (Mflop/s)
smatv-intf	52.50	597.3
smatv-tetra	25.40	536.8
PCG-block	19.10	82.2
Others	3.00	-

The code achieved good vectorization on the CRAY T90 for a mesh with 8750 elements, comprising 4419 interface and 4331 tetrahedra. The top three subroutines are responsible for major CPU utilization in the whole analysis.
The parallel performance is shown in table 2 and the figures 7 (a) and (b) give a summary report provided ATEXPERT, the autotasking performance tool. The top five subroutines assigned for parallel analysis are presented in tab. 2. The routines **Fint-tetra** and **Fint-intf** evaluate respectively the internal force vector of the interface and tetrahedra elements. The routine **Kintf** computes the stiffness matrices for the interface elements.

Table 2: Summary of the ATEXPERT's Report for the 5 dominant loops

Routines	% Parallel	Dedicated Speedup	Actual Speedup
Smatv-tetra	98.9	3.96	3.8
Smatv-intf	99.8	3.83	3.8
Fint-tetra	92.5	3.83	3.2
Fint-intf	99.1	3.55	3.5
Kintf	85.8	3.53	2.6

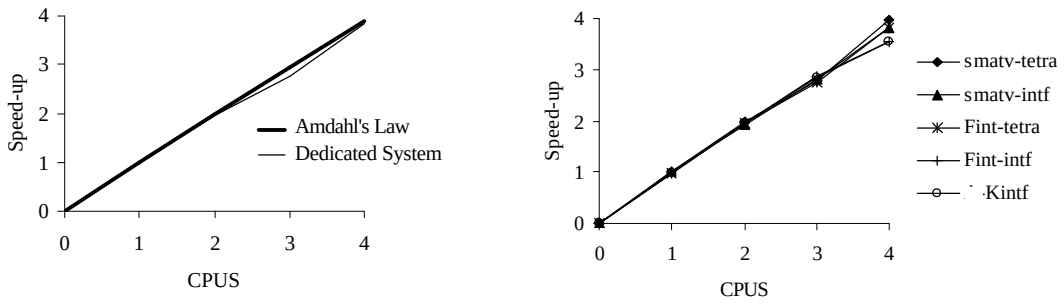

(a) (b)

Figure.7: (a) Program Summary of the ATEXPERT's Report
(b) ATEXPERT's Report -The top 6 subroutines on a Dedicated Speedup

According to ATEXPERT tool this program appears to be 99.2 percent parallel and 0.8 percent serial. Amdahl's Law predicts the program could expect to achieve a 3.9 times speedup on 4 cpus.

6 Concluding remarks

This paper presented the optimized implementation of Rossi's a probabilistic model for the simulation of cracking in concrete structures. This model in based on the assumption that some particularities of the cracking behavior of concrete, such as strain softening, cracking evolution and size-effects are derived from the heterogeneous characteristics of the material.

The probabilistic methodology presented in this paper corresponds to the 3D analysis of a strongly nonlinear material that develops cracking. In adition, the finite elements analysis must be called several times within a Monte Carlo simulation. Therefore, the code needs to be optimized in such a way that the simulation time does not exceed a practical limit. The example presented in this paper shows that the model is capable of simulating the crack opening and the crack pattern.

The code achieved a very good level for both parallel performance and vetorization. The most demanding routines, which implement the matrix-vector-multiply computational kernel for the interface and tetrahedral elements, are "fully" parallelized (~ 99%) and responsible for over 80% of CPU time. The results emphasizes the suitability of the implemented code on the parallel-vector machine, CRAY T90 for 2 CPU's, which presented a flop rate of 614 Mflop/s and a parallel speed-up of 3.8 for 4 CPU's.

Extensive use of element-by-element techniques within the computational kernels comprised in the iterative solution drivers provided a natural way for achieving high Flop rates and good parallel speed-up's. Furthermore, element-by-element techniques, avoid completely the formation and handling of large sparse matrices. Therefore, the computational strategies presented herein provide a natural way to deal with more complex scenarios, particularly those involving three-dimensional problems.

Acknowledgments

The authors are indebted to the Computer Graphics Technology Group TECGRAF/PUC-Rio, High Performance Computing Center NACAD/COPPE/UFRJ, and the Laboratory of Computa-

tional Methods in Engineering of the Program of Civil Engineering LAMCE /COPPE/UFRJ. CESUP/UFRGS is gratefully acknowledged for the computer time provided for the performance experiments.
This work was partially supported by CAPES and CNPq's grant N° 150039/01-8(NV).

References

[1] P. Rossi, X. Wu, F. le Maou, and A. Belloc, *Scale effect on concrete in tension*. Materials and Structures, 27 (172), (1994), 437-444.

[2] C. N. M. Paz, *Development and Implementation Probabilistic Model for 2D and 3D Discrete Cracking Concrete in Parallel Computing*, D.Sc. Thesis, COPPE/UFRJ, the Graduate Institute of Federal University of Rio de Janeiro, Brazil (2000) [in Portuguese].

[3] W. H. Press, S. Teukolski, W.T. Vetterling and B. Flannery, *Numerical Recipes*, Cambridge University Press (1992).

[4] E. M. R. Fairbairn, C. N. M. Paz, N. F. F. Ebecken, and F-J. Ulm, *Use of neural network for fitting of probabilistic scaling model parameter*, Int. J. Fracture, 95, (1999), 315-324.

[5] E. M. R. Fairbairn, N. F. F. Ebecken, C. N. M. Paz and F-J. Ulm, *Determination of probabilistic parameters of concrete: solving the inverse problem by using artificial neural networks*, Computers and Structures, 78, (2000), 497-503.

[6] E. M. R. Fairbairn, V.J.C. Debeux, C. N. M. Paz and N. F. F. Ebecken, Applications of probabilistic Aproach to the Analisysis of gravite Dam Centrifuge Test, 8th ASE Specialty Conference on probabilistic Mechanics and Structural Reability (2000) PMC 200-216.

[7] C. T. Kelley, *Iterative Methods for Linear and Nonlinear Equations.* Frontiers in applied mathematics, SIAM Society for Industrial and Applied Mathematics, Philadelphia, (1995).

[8] T. J. R. Hughes, R. M. Ferenez, J. O. Hallquist, *Large-Scale Vectorized Implicit Calculation in Solid Mechanics on a CRAY X-MP/48 Utilizing EBE Preconditionated Conjugate Gradients* Computer Methods in applied Mechanics and Engineering, 61, (1987), 2115-248.

[9] M. Papadrakakis, *Solving Large-Scale Problems in Mechanics: The Development and Application of Computational Solution*, Editor, M. Papadrakakis, John Wiley and Sons, (1993).

[10] F.E. Amparano, X.Yunping and R. Young-Sook, *Experimental stydy on the effect of agregate contents on fracture behavior of concrete*, Engineering Fracture Mechanics 67 (2000), 65-84.

[11] L.C.G. Coelho, M. Gattass, L.H. de Figueiredo, *Intersecting and Trimming Parametric Meshes on Finite-Element Shells.* International Journal for Numerical Methods in Engineering; 47(4), (2000), 777-800.

[12] J.B. Cavalcante Neto, P.A. Wawrzynek, M.T.M. Carvalho, L.F. Martha, A.R. Ingraffea, *An Algorithm for Three-dimensional Mesh Generation forArbitrary Regions with Cracks*, Engineering with Computers; 17(1), (2001), 75-91.

[13] A.L.Coutinho, M.A. Martins, J.L.D. Alves, L. Landau, and A. Moraes, *Edge-based finite element tecniques for nonlinear solid mechanics problems*. Int. J. for Numerical Methods in Engineering, 50 (9), (2001) 2050-2068.